ACS OMEGA

Open Access

http://pubs.acs.org/journal/acsodf

Article

Iron-Based Catalysts Derived from Iron-Containing Sludge for Enhanced Catalytic Performance of H_2S Selective Catalytic Oxidation

Runtian He, Xiaoyu Zhang, Jia-nan Gu, Kan Li, Mingming Guo,* Fangming Jin,* Jinping Jia, and Tonghua Sun

Cite This: *ACS Omega* 2024, 9, 29691−29699

Read Online

ACCESS | Metrics & More | Article Recommendations

ABSTRACT: In this work, iron-containing sludge is used to prepare iron-based catalysts for efficient H_2S selective catalytic oxidation. First, the effect of calcination temperatures on the catalytic activities of H_2S selective oxidation is carried out and it can be found that S-500 calcined at 500 °C performs excellent catalytic activity. Then, the catalytic performance of the S-500 catalyst is further optimized using alkaline treatment with different concentrations of NaOH solution. The results indicate that S-500(2.0) treated with 2 M NaOH solution has the highest catalytic activity of H_2S selective oxidation. Next, various characterization methods are used to analyze the structure and physical-chemical of the sludge-based catalysts. N_2-Brunauer−Emmett−Teller (N_2-BET) and X-ray photoelectron spectroscopy analyses show that the S-500(2.0) catalyst has the smallest average particle (11.17 nm), the biggest ratio of S_{ext}/S_{micro}(17.98) with bigger external specific surface area (49.09 $m^2 \cdot g^{-1}$), a higher proportion of Fe^{3+} species (50.88%), and surface adsorbed oxygen species (48.07%). Meanwhile, O_2-TPD and CO_2-TPD analysis indicates that the S-500(2.0) catalyst has a bigger value of the O_{ads}/O_{Total} ratio (50.56%) and $(CO_2)_{(weak+moderate)}$ /$(CO_2)_{Total}$ ratio of (31.41%), indicating that there are much more oxygen vacancies and weak alkaline sites. As a result, the excellent catalytic performance of H_2S selective oxidation can be attributed to its outstanding physical−chemical properties.

1. INTRODUCTION

In recent years, with the increase in the use of chemical raw materials and industrial additives in chemical synthesis, it has become increasingly difficult to treat industrial wastewater.[1−3] Faced with the raised emission standards, traditional secondary biochemical treatment can no longer meet the new emission requirements. Therefore, it is necessary to add some advanced treatment to meet the new high-standard emission requirements.[4,5] Among them, Fenton oxidation technology was widely used in deep treatment.[6] After the oxidation reaction is completed, alkali is added to neutralize the coagulated iron ions to remove pollutants. Therefore, after long-term operation of the combined Fenton oxidation-biochemical treatment of industrial wastewater, residual activated sludge would be produced and a large amount of iron-containing sludge would also be accompanied.[7,8] According to the literature, the average mud production of iron-containing sludge is 4.1 g/L.[9] While the direct leak of untreated sludge leaks into water or soil will result in environmental pollution, it can increase the risk of disease transmission.[10] Therefore, reasonable disposal techniques must be adopted to reduce the potential hazards of sludge.

At present, traditional treatment and disposal methods of sludge mainly include incineration, landfill, and composition of building materials.[10] However, traditional technologies are mainly focused on the dehydration, reduction, or transfer of pollutants. Therefore, it is urgent to develop high-value-added and resource-utilization technology of sludge.[11,12] Based on the fact that the main components of dried sludge after high-temperature calcination are SiO_2, AlO_x, FeO_x, and some organic functional groups, it is reasonable to prepare some catalysts using these active substances in the sludge and can be used for the catalytic degradation of organic matters in sewage, desulfurization, and denitrification.[5,11−14] Since the catalyst is a high-value-added product, harmful solid waste can be widely used as an efficient catalyst of pollutant degradation after appropriate treatment.[12,13]

Hydrogen sulfide (H_2S) is a typical malodorous gas with a wide range of sources such as crude oil processing, coal gas generation, and coal-fired power plants.[15] In addition, H_2S can be easily oxidized into SO_2 and secondary pollutants such as acid rain can be formed, which can cause serious pollution to the

Received: April 1, 2024
Revised: June 7, 2024
Accepted: June 14, 2024
Published: June 26, 2024

environment.[16,17] Therefore, many researchers have paid much more attention to developing efficient treatment technology of H_2S.[17,18] At present, the main treatment methods for H_2S can be divided into absorption, adsorption, biotrickling filtration, and catalytic oxidation method.[18−22] Among them, most of the absorption and adsorption methods cannot be applied to the precise removal of H_2S in different concentrations. By comparison, the catalytic oxidation method has the advantages of large-capacity gas processing, high performance of desulfurization, wide applicability, and less secondary pollution.[18−20] The principle of the catalytic oxidation method is the catalytic oxidation of H_2S into sulfur in the presence of oxygen. The reaction formula is as follows:

$$H_2S + \frac{1}{2}O_2 \rightarrow \frac{1}{n}Sn + H_2O$$

Metal oxide-based catalysts are widely used in the removal of H_2S by catalytic oxidation. Common catalysts include Fe_2O_3, CuO, ZnO, rare earth metal-based, and various composite metal-based catalysts.[20,23,24] In addition, activated carbon, SiO_2, Al_2O_3, TiO_2, and other materials with large specific surface areas and good porous materials are used as carriers to improve the structural disadvantages of metal oxides and prevent sintering and aggregation, thereby improving its catalytic performance.[23,25] Due to the presence of iron-based active compounds, the sludge can be used to prepare the catalysts of H_2S selective oxidation. At the same time, the porous materials such as SiO_2 contained in sludge may improve the specific surface areas of the catalysts.[23] Therefore, in this work, the iron-containing sludge and remaining sludge produced in the treatment of industrial wastewater are selected as the research object, and iron-based catalysts are prepared by calcining treatment and alkaline treatment. First, the effects of different calcination temperatures and alkali concentrations on the catalytic performance of H_2S degradation on the sludge-based catalysts are investigated. Then, the catalytic evaluation in an atmosphere with water vapor and without water vapor is carried out to evaluate the catalytic stability of the optimized catalyst. At last, the composition, surface morphology, and physical−chemical properties of the catalyst were characterized. Moreover, the structure−activity relationship between the catalysts and their catalytic activities of H_2S oxidation are explored.

2. EXPERIMENTAL SECTION

2.1. Materials and Reagents. The sludge used in this work was obtained from a renewable energy plant in Shanghai, China, and the dewatered sludge was used as the raw sludge. All other reagents used in this work were analytical grade and no further treatment was operated.

2.2. Catalyst Preparation Calcined with Different Temperatures. First, a series of catalysts calcined at different temperatures (300, 400, 500, 600, and 700 °C) using the dried sludge as a precursor are synthesized and the specific method is as follows. A certain amount of dried sludge sample was taken and placed in the muffle furnace at a heating rate of 5 °C·min^{-1} to the target temperature and maintained for 3 h. After cooling, the samples were ground and sieved again to obtain a sludge-based catalyst with 40−60 mesh samples. Based on the corresponding calcined temperature, the obtained catalysts are marked $S-T$ (T = 300, 400, 500, 600, and 700) catalysts.

2.3. Catalyst Preparation Treated with NaOH Solution. In order to explore the effect of alkali modification on their catalytic activities of H_2S oxidation, a series of catalysts treated using different concentrations of NaOH solution were prepared. First, a certain amount of S-500 was impregnated into 10 mL of NaOH solution with different concentrations for 8 h. Then, the above mixture was filtered, washed, and dried in the oven at 105 °C overnight. Next, the dried samples were raised to 500 °C at a heating rate of 5 °C·min^{-1} in a muffle furnace and kept for 3 h. After cooling, grinding, and sieving again, the catalysts with 40−60 mesh were obtained and the catalyst was named S-500(C), C = 0.1, 0.5, 1.0, 2.0, and 4.0 catalyst according to the alkali concentration.

2.4. Desulfurization Performance Test. The test system of desulfurization performance includes a gas distribution system, reaction system, and detection system. Among them, the gas simulation experiment is composed of the mixed gas of N_2, H_2S, and O_2 through the mass flow control, and the inlet and outlet concentrations of H_2S are analyzed by gas chromatography. Then, 0.2 g of sample is loaded into a quartz tube reactor, fixed with quartz wool to prevent the catalyst from being blown away. The reaction temperature is adjusted and controlled through a temperature controller. In this work, the flow rate and the inlet concentration of H_2S are controlled at 50 mL·min^{-1} and 200 mg·m^{-3}, respectively. The stable experiment with H_2O and without H_2O is terminated until the outlet concentration of H_2S exceeds 20 mg·m^{-3}. H_2S was analyzed on Agilent-7890B (FPD detector) gas chromatography. The water content is analyzed by a portable hygrometer and the concentration of O_2 is analyzed by a Haixin GC-950 (TCD detector) gas chromatography. H_2S removal efficiency and S selectivity were defined according to the following equations:

$$H_2S \text{ removal efficiency} = \frac{[H_2S]_{in} - [H_2S]_{out}}{[H_2S]_{in}} \times 100\%$$

$$S_{selectivity} = \frac{[H_2S]_{in} - [H_2S]_{out} - [SO_2]_{out}}{[H_2S]_{in} - [H_2S]_{out}} \times 100\%$$

$[H_2S]_{in}$ and $[H_2S]_{out}$ are the inlet and outlet concentrations of H_2S (ppm), respectively. where $[SO_2]_{out}$ is the outlet concentration of SO_2 (ppm).

2.5. Catalyst Characterization. In this work, the physicochemical properties of the prepared catalyst were characterized using relevant instruments. X-ray fluorescence spectroscopy (XRF) is used to investigate the types and relative contents of elements in the samples; the X-ray diffraction (XRD) pattern of the catalyst is obtained using the Shimazu XRD-6100 diffractometer to analyze the phase structure of the catalyst; N_2 adsorption−desorption isotherms of the catalyst is carried out using TriStar II 3020 to obtain the specific surface area and pore size distribution of the catalyst; the Brunauer−Emmett−Teller (BET) and the t-plot method was used to calculate the specific surface area (S_{BET}), the surface area (S_{EXT}) and micropore volume (V_{Micro}), respectively. Scanning electron microscopy (SEM) is completed to observe the surface structure of the catalyst using the FEI Quanta 400 FEG; inductively coupled plasma atomic emission spectrometry (ICP-AES) is tested to obtain the detailed content of metal elements in the sample; X-ray photoelectron spectroscopy (XPS) is carried out to get the surface elemental composition of the catalyst using Thermo ESCALAB 250XI instrument equipped with monochromatic Al Kα; temperature-programmed desorption testing with CO_2/O_2 as the attached gas is used to analyze the types of surface bases and oxygen species of catalysts using AutoChem II 2920 chemical adsorption instrument.

https://doi.org/10.1021/acsomega.4c03115
ACS Omega 2024, 9, 29691−29699

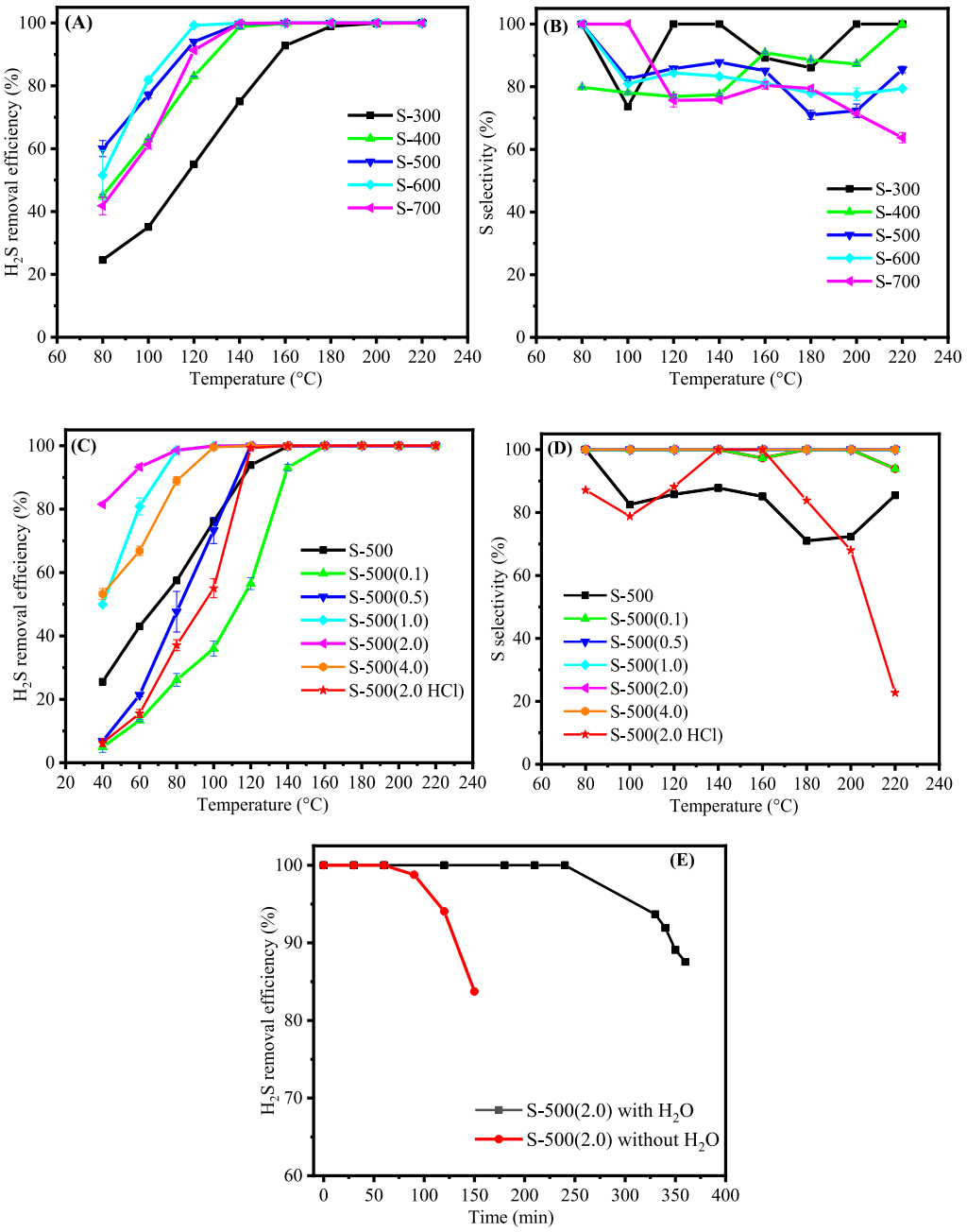

Figure 1. Desulfurization performance on the catalysts prepared at different calcination temperatures (A, B); the catalysts prepared treated with different concentrations of alkali (C, D); catalytic stability with water and without water (E).

3. RESULTS AND DISCUSSION

3.1. Desulfurization Performance. To investigate the effect of calcination temperature on the catalytic performance of H_2S selective oxidation on the sludge-based catalysts prepared at 300, 400, 500, 600, and 700 °C, a series of tests were carried out and the results are shown in Figure1A, B. The results showed that the catalytic activities increased with the increase of calcination temperature during 300−600 °C, while the catalytic performance of the catalyst calcined at 700 °C had a significant decline. Among them, the activity of S-600 prepared at 600 °C was similar to that of S-500 prepared at 500 °C. Overall, the descending order of H_2S removal efficiency was as follows: S-(600) > S-(500) > S-(400) > S-(700) > S-(300). Moreover, worse *S* selectivity around 75% can be seen on *the S−T* catalyst. Therefore, 500 °C was selected as the optimized calcination

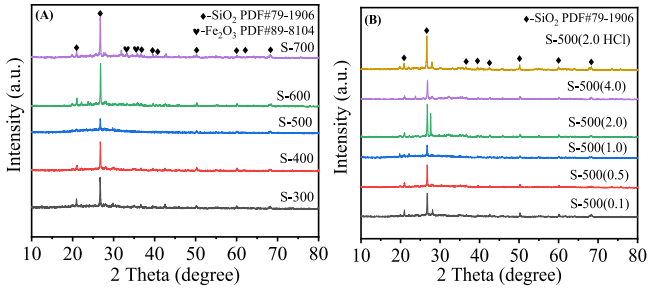

Figure 2. XRD spectra of sludge-based catalysts obtained by different calcination temperatures (A) and treated with different concentrations of alkali solution (B).

https://doi.org/10.1021/acsomega.4c03115
ACS Omega 2024, 9, 29691−29699

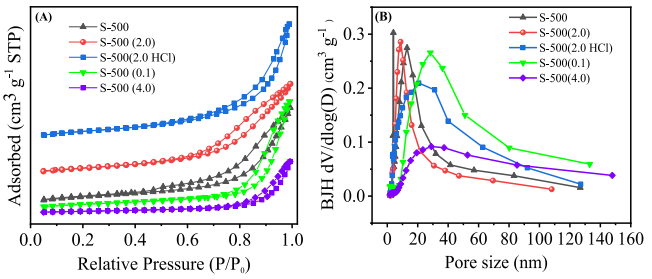

Figure 3. N_2 adsorption−desorption isotherms (A) and pore size distribution (B) of sludge-based catalysts.

temperature with lower energy consumption and used as a representative for subsequent acid and base modification.

In order to further improve the catalytic performance of H_2S selective oxidation on the S-500 catalyst, the influence of alkali concentrations (0.1−4 mol/L) on their catalytic performance was investigated as shown in Figure 1C, D. By comparison, it was found that the S-500(2.0).

The catalyst treated with 2 mol/L NaOH solution performed the best performance of H_2S selective catalytic oxidation, while the S-500(0.1) catalyst treated with 0.1 mol/L NaOH solution had the worst catalytic activity. It can be seen that compared with the untreated catalysts, the performance of the sludge-based catalysts impregnated with NaOH solution had been improved to varying degrees. In addition, a 2 M HCl solution was used to treat the S-500 catalyst to make a comparison with S-500(2.0), and the S-500(2.0 HCl) catalyst performed worse performance than that of S-500(2.0). Among them, the H_2S removal efficiency of S-500(1.0), S-500(2.0), and S-500(4.0) can reach 100% at 100 °C of reaction temperature, while S-500 catalyst needed above 140 °C to reach 100% removal efficiency. The H_2S removal efficiency of S-500(2.0) can still reach above 90% at 80 °C of reaction temperature. More importantly, the S selectivity of S-500(C) catalysts except for S-500(0.1) had raised to 100% and the S selectivity of S-500(0.1) is significantly improved compared to the S-500 catalyst.

Meanwhile, the stable experiment of H_2S selective catalytic oxidation was completed at 100 °C of reaction temperature, as shown in Figure 1E. The activity of H_2S removal efficiency on the S-500(2.0) catalyst began to decrease after 250 min in an atmosphere with water vapor, and the H_2S removal efficiency dropped below 90% after 360 min. While the performance of H_2S efficiency on S-500(2.0) began to decline after about 90 min without water vapor, and the removal efficiency decreased below 90% after about 130 min. It can be seen that the presence of water vapor contributed to improving the desulfurization performance of H_2S selective catalytic oxidation on the S-500(2.0) catalyst. This result is also in line with the recognized mechanism of H_2S selective catalytic oxidation, which is a liquid−solid−gas three-phase reaction. In the presence of water vapor, the gas phase of H_2O is first adsorbed on the surface of the catalyst and a layer of water film is formed. Then, H_2S and O_2 molecules are dissolved into the water film, and they are dissociated into HS- and active oxygen atoms, respectively.

3.2. XRD Analysis. Figure 2A shows the XRD diffraction patterns of sludge-based catalysts prepared at different calcination temperatures. There are some diffraction peaks at 2θ = 20.9, 26.8, 36.6, 39.5, 40.4, 42.8, and 50.3, 59.9, and 68.2° belong to the SiO_2 phase [PDF# 79-1906] on the $S-T$ samples below 500 °C. As the calcination temperature increased from 300 to 500 °C, the intensity of these diffraction peaks gradually

Table 1. Specific Data of XRF, N_2-BET, and XPS Result on the Sludge-Based Catalysts

	XRF result					N_2-BET						XPS result				
sample	Fe	Si	Al	Ca	K	d_{BJH}	S_{BET}	S_{Ext}	S_{Micro}	V_{total}	S_{ext}/S_{micro}	Fe	Si	Al	Ca	K	O
			wt %			nm	$m^2 \cdot g^{-1}$	$m^2 \cdot g^{-1}$	$m^2 \cdot g^{-1}$	$cm^3 \cdot g^{-1}$		wt %					
S-500	12.71	9.99	6.71	8.96	1.90	12.22	71.76	50.67	21.09	0.194	2.40	1.85	5.39	8.62	2.65	0.67	48.13
S-500(0.1)	12.38	10.91	6.33	8.68	1.72	20.04	43.05	35.44	7.61	0.200	4.66	2.66	6.04	12.84	2.95	0.77	52.19
S-500(2.0)	13.73	11.05	2.98	9.659	1.49	11.17	51.82	49.09	2.73	0.173	17.98	3.41	7.34	6.85	6.02	0.92	57.17
S-500(4.0)	15.77	10.91	3.10	10.509	1.55	23.06	16.09	13.79	2.30	0.092	6.00	4.16	5.96	6.61	6.32	0.90	58.14
S-500(2.0 HCl)	14.81	6.93	2.87	2.379	1.61	13.25	59.16	55.51	3.65	0.217	15.20	2.69	10.85	10.09	1.29	0.98	57.64

https://doi.org/10.1021/acsomega.4c03115
ACS Omega 2024, 9, 29691−29699

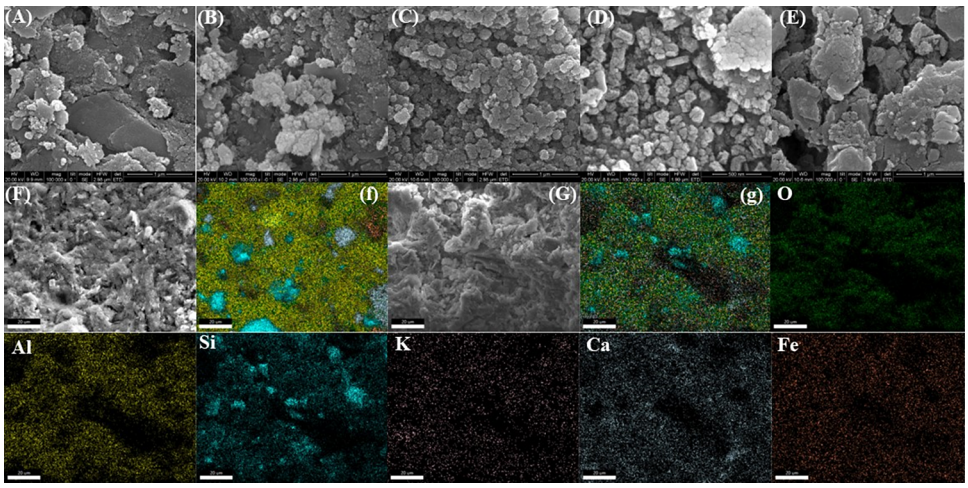

Figure 4. SEM images of S-500 (A), S-500(0.1) (B), S-500(2.0) (C), S-500(4.0) (D), S-500(2.0 HCl) (E), element overlay of S-500 (F, f), S-500(2.0) (G, g) and EDS of S-500(2.0).

became weakened, and a weak diffraction peak at $2\theta = 26.8°$ can be seen on the S-500 catalyst, indicating that the SiO_2 crystals in the S-500 catalyst may be in an amorphous state. As the calcination temperature further increased, the diffraction peaks belonging to SiO_2 began to become stronger again, and some diffraction peaks at $2\theta = 33.2$ and 35.8° assigned to Fe_2O_3 [PDF # 89-8104] began to appear. This indicated that other components are highly dispersed on the surface of SiO_2 in the catalysts prepared at lower calcination temperatures. With the calcination temperature increase, metal oxides such as Fe_2O_3 began to appear on the surface of the samples. Figure 2B shows the XRD spectrum of the sludge-based catalysts treated with different concentrations of alkali solution. It can be seen that the modification of the alkali solution had no obvious effect on the crystal structure of the catalysts. The intensity of diffraction peaks on the S-500(2.0) catalyst impregnated with 2 M NaOH solution was higher than that of other concentrations of alkali solution, indicating that alkaline impregnation is beneficial for the crystallization of SiO_2. Overall, it can be seen that the main crystal phase of the sludge-based catalysts is mainly composed of SiO_2 and Fe_2O_3.

3.3. N_2 BET and Surface Morphology. From Figure 3A, it can be seen that all N_2 adsorption−desorption isotherms on sludge-based catalysts exhibited typical Type IV with the hysteresis loop, indicating that sludge-based samples are typical of mesoporous materials.[17,26] From Table 1, it can be seen that the specific surface area of S-500, S-500(0.1), S-500(2.0), S-500(4.0), and S-500(2.0 HCl) was 71.76, 43.05, 51.82, 16.09, and 59.16 $m^2\ g^{-1}$, respectively. It can be seen that the alkali or acid treatment can result in the decrease of the specific surface area on the sludge-based catalysts. High concentration of NaOH solution can lessen the S_{BET} value of S-500(4.0) to 16.09 $m^2\ g^{-1}$. In addition, the external specific surface area of S-500, S-500(0.1), S-500(2.0), S-500(4.0), and S-500(2.0 HCl) was 50.67, 35.44, 49.09, 13.79, and 55.51 $m^2\ g^{-1}$, respectively. Moreover, the S_{ext}/S_{micro} values of S-500, S-500(0.1), S-500(2.0), S-500(4.0), and S-500(2.0 HCl) are 2.40, 4.66, 17.98, 6.00, and 15.20, respectively. By comparison, S-500(2.0) has the biggest value of S_{ext}/S_{micro} and the bigger external specific surface area was in favor of the adsorption and diffusion of H_2S molecules, resulting in the improvement of H_2S selective catalytic oxidation on S-500(2.0). In addition, the total pore volume of S-500(2.0) decreased from 0.194 to 0.173 $cm^3 \cdot g^{-1}$, while the value of S-500(2.0 HCl) increased from 0.194 to 0.217 $cm^3 \cdot g^{-1}$. The possible reason is that alkaline impregnation may block the pores. From Figure 3B, it can be seen that the S-500(2.0) catalyst has a smaller average particle size than those of S-500, S-500(0.1), S-500(4.0), and S-500(2.0 HCl). Furthermore, from Table 1, it can be found that the average particle size of S-500, S-500(0.1), S-500(2.0), S-500(4.0), and S-500(2.0 HCl) was 12.22, 20.04, 11.17, 23.06, and 13.25 nm, respectively. In general, the surface of the catalyst with the smaller particles was beneficial to the enrichment of more active sites, resulting in the enhancement of the catalytic activity of H_2S oxidation.

In order to further analyze the surface microstructure of the sludge-based catalysts, SEM characterization was performed and Figure 4 shows the surface morphology of S-500, S-500(0.1), S-500(2.0), S-500(4.0), and S-500(2.0 HCl) catalysts. Figure 4A, B shows that the surface morphology of S-500 and S-500(0.1) catalysts was irregular and their surface pore structure is poor. From Figure 4C, it can be observed that particles are evenly distributed and dispersed on the surface of the S-500(2.0) catalyst. As shown in Figure 4D, nonuniform particles with obvious agglomeration can be observed on the surface of the S-500(4.0) catalyst. As for the S-500(2.0 HCl) catalyst, loose and indistinct blocky substances can be seen on its surface. In order to further determine the elements and content on the surface of the S-500 and S-500(2.0) catalyst, energy spectrum analysis was performed, as shown in Figure 4 and Table 2. It can be seen that the elements including Fe, Si, Al, Ca, K, and O were present on the surface of S-500 and S-500(2.0) catalysts. As shown in Table 2, the weight ratios of Fe (12.76%), Si (14.44%), and Ca (13.49%) on the S-500(2.0) catalyst are higher than those of Fe (8.87%), Si (13.19%), and Ca (10.78%) on S-500 catalyst, while the weight ratio of Al (18.57%) on the S-500(2.0) catalyst is lower than that of Al (11.12%) on the S-500 catalyst. This result was in line with the XRF, ICP, and XPS analysis, indicating that the treatment of NaOH solution can improve the amount of Fe, Si, and Ca and lessen the number of Al.

3.4. O_2-TPD/CO_2-TPD Analysis. The catalytic activity of H_2S selective oxidation is closely related to its activated ability of oxygen on the sludge-based catalysts. O_2-TPD technology was carried out to determine the desorption amount of different oxygen species in the catalysis, as shown in Figure 5A. It is generally believed that oxygen can be activated through the conversion process of $O_2 \rightarrow O_2^- \rightarrow O_2^{2-} \rightarrow O^- \rightarrow O^{2-}$. Due to

https://doi.org/10.1021/acsomega.4c03115
ACS Omega 2024, 9, 29691−29699

Table 2. Results of ICP, EDS, and XPS Analysis on the Sludge-Based Catalysts

	ICP result					EDS result						XPS analysis			
	Fe	Si	Al	Ca	K	Fe	Si	Al	Ca	K	O	Fe^{3+}	Fe^{2+}	Fe^{3+}/Fe^{2+}	O_{ads}	O_{latt}	O_{ads}/O_{latt}
sample	wt %					wt %						%			%		
S-500	4.89	13.15	7.03	3.26	13.15	8.87	13.19	18.57	10.78	1.66	46.92	46.03	53.97	0.85	43.35	37.51	1.15
S-500(0.1)												47.41	52.59	0.90	36.11	36.49	0.99
S-500(2.0)	8.73	17.19	7.07	6.35	1.78	12.76	14.44	11.12	13.49	1.71	46.47	50.88	49.12	1.04	48.07	29.18	1.65
S-500(4.0)												48.66	51.34	0.95	42.28	35.74	1.19
S-500(2.0 HCl)	7.67	15.64	9.59	1.76	1.86							47.29	52.71	0.90	43.91	39.64	1.10

the fact that O_2, O_2^-, and O_2^{2-} species desorbed at similar temperatures, it is difficult to distinguish them based on their desorption temperature. Therefore, the desorption peak at low temperatures can be attributed to the desorption of chemically adsorbed oxygen (O_{ads}, including O_2, O_2^-, and O_2^{2-}) species, while the desorption peak at medium to high temperatures and high temperatures can be assigned to the desorption of surface lattice oxygen (O_{latt}), and bulk lattice oxygen, respectively.[17,26] From Figure 5A, it can be observed that the sludge-based catalysts were composed of three oxygen desorption peaks. The desorption peaks at 30−300 and 300−500 °C were due to the desorption of surface adsorbed oxygen species (O_{ads}) and surface lattice oxygen (O_{latt}), while the desorption peaks above 500 °C were due to the desorption of bulk lattice oxygen species in the sludge-based catalysts. Meanwhile, the related desorbed amount of oxygen species including O_{ads} and O_{latt} on the catalysts is listed in Table 3. Moreover, the value of O_{ads}/O_{Total} ($O_{Total} = O_{ads} + O_{latt}$) ratio was calculated and the ratios of S-500, S-500(0.1), S-500(2.0), and S-500(4.0) were in the descending order of S-500(2.0) (50.56%) > S-500(4.0) (43.52%) > S-500(0.1) (26.79%) > S-500 (25.44%). It can be seen that the S-500(2.0) sample has the biggest ratio of adsorbed oxygen on its surface, suggesting that there are much more oxygen vacancies on the S-500(2.0) catalyst, which is consistent with its best catalytic activity of H_2S selective oxidation.

According to the reports, the alkaline sites on the surface of the catalyst play a crucial role in the selective catalytic oxidation of H_2S.[17] In general, the H_2S molecule needed to be dissociated into HS^- on the alkaline sites before it can be further oxidized, while alkaline sites can promote this dissociation reaction, thus promoting its desulfurization performance.[17,26] Moreover, the large amount of elemental S generated during H_2S selective catalytic oxidation contributed to increasing the colliding and merging probability of S atoms with each other, making it easier to form cyclic or chain-shaped S8 structures, which can be easily precipitated. As a result, it can be avoided to further oxidize into SO_2, thus improving the *S* selectivity of the catalyst. In order to analyze the surface alkalinity of the sludge-based catalyst, CO_2-TPD characterization was performed on S-500, S-500(0.1), S-500(2.0), and S-500(4.0) catalysts treated with different concentrations of NaOH solution, as shown in Figure 5B. As shown in the figure, the peaks below 300 °C can be defined as a weakly alkaline site, which was related to the presence of hydroxyl groups on the surface of the catalyst. The desorption peaks located at 300−500 °C and above 500 °C belong to the moderately alkaline position and the strong alkaline sites, respectively.[17,26] In general, weak or moderate alkaline sites were beneficial to the adsorption and dissociation of H_2S, and the desorption of sulfur product; strong alkaline sites may have an adverse effect on the desorption of sulfur product, further resulting in the generation of sulfate byproducts. In addition, the desorbed amount of CO_2 and the $(CO_2)_{(weak+moderate)}/(CO_2)_{Total}$ ratios are listed in Table 3. By comparison, the S-500(2.0) catalyst treated with a 2 M NaOH solution had the biggest ratio of $(CO_2)_{(weak+moderate)}/(CO_2)_{Total}$ with 31.41%, indicating that S-500(2.0) had a larger proportion of weak or moderate alkaline sites on its surface, which was conducive to the adsorption/dissociation of H_2S and the desorption of sulfur.

3.5. XPS Analysis. In order to further determine the elemental composition and valence state on the surface of sludge-based catalysts, X-ray photoelectron spectroscopy (XPS) testing was performed on the samples. The binding energies (BEs) of other elements were calibrated using the peak of C 1s at

https://doi.org/10.1021/acsomega.4c03115
ACS Omega 2024, 9, 29691−29699

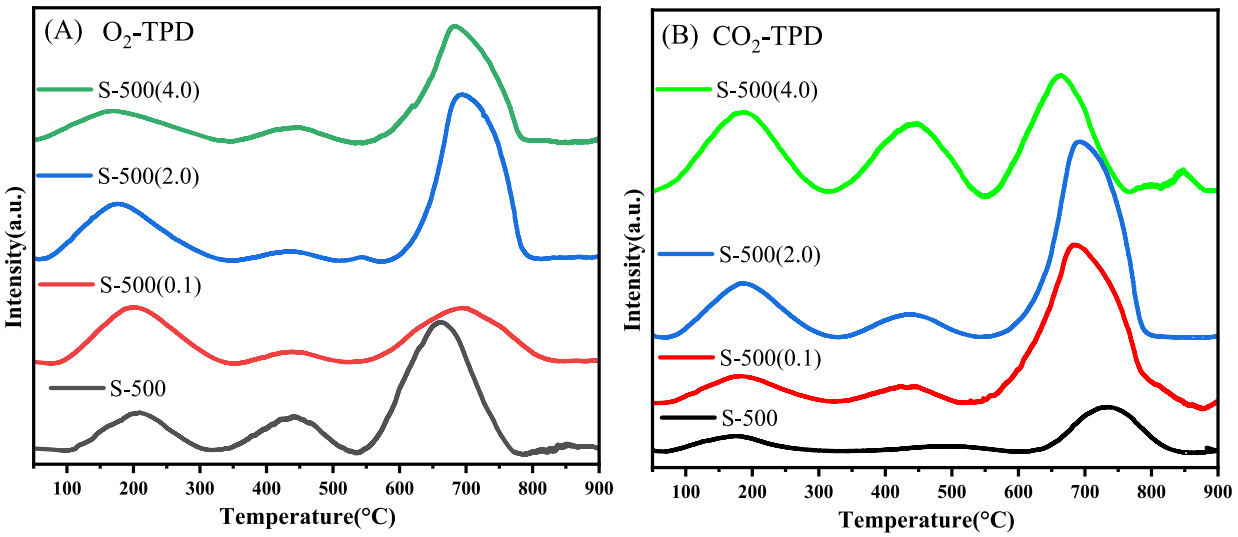

Figure 5. O_2-TPD(A) and CO_2-TPD(B) of S-500, S-500(0.1), S-500(2.0), and S-500(4.0).

Table 3. Desorbed Amount of O_2 and CO_2 on the Sludge-Based Catalysts

	O_2-TPD			CO_2-TPD			
	30−300 °CSi	300−500 °C Ca		30−300 °C Si	300−500 °C Ca	500−900 °C	
	O_{ads}	O_{latt}	O_{ads}/O_{Total}	$(CO_2)_{weak}$	$(CO_2)_{moderate}$	$(CO_2)_{strong}$	$(CO_2)_{(weak+moderate)}/(CO_2)_{Total}$
sample	mmol/g		%	mmol/g			%
S-500	0.361	1.058	25.44	0.053	0.067	0.636	15.87
S-500(0.1)	0.176	0.481	26.79	0.160	0.405	2.665	17.49
S-500(2.0)	0.403	0.394	50.56	0.278	0.294	1.249	31.41
S-500(4.0)	0.457	0.593	43.52	0.387	0.828	4.649	20.72

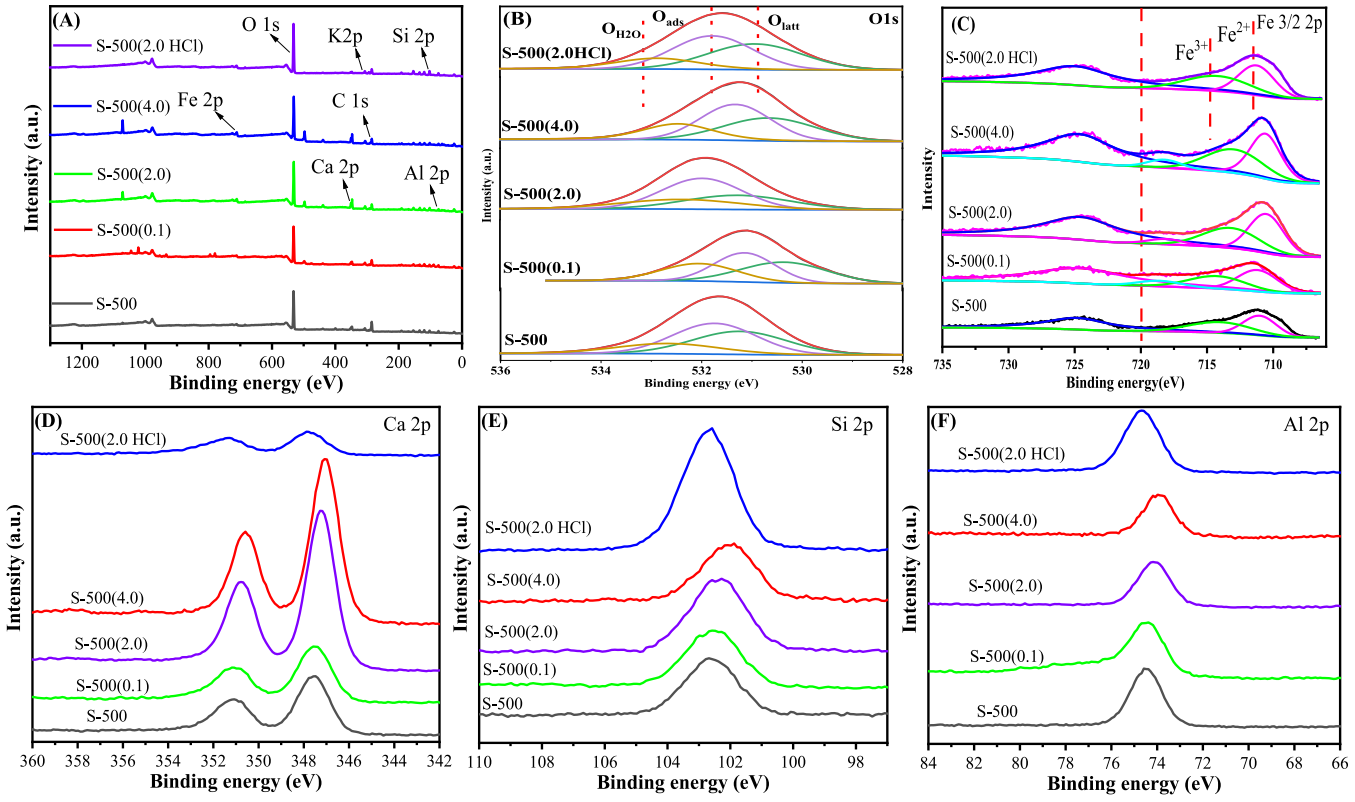

Figure 6. XPS survey (A); O 1s spectra (B); Fe3/2 2p spectra (C); Ca 2p spectra (D); Si 2p spectra (E) and Al 2p spectra (F).

https://doi.org/10.1021/acsomega.4c03115
ACS Omega 2024, 9, 29691−29699

284.8 eV and the XPS spectrum is illustrated in Figure 6. From Figure 6A, it can be seen that the peaks of Fe, Si, Al, Ca, K, and O elements are accurately identified in the full scan of the XPS spectrum, and the approximate content of the elements is shown in Table 1, indicating that the sludge-based catalysts were composed of multi-elements. As shown in Figure 6B, the fine spectrum of O 1s mainly includes surface lattice oxygen species (O_{latt}) at BE = 530.9 eV, surface-adsorbed oxygen species (O_{ads}) at BE = 531.7 eV, hydroxy oxygen species at BE = 533.1 eV.[17,26,27] According to the literature,[17] surface-adsorbed oxygen with high mobility is the most active species in selective catalytic oxidation of H_2S, and the number of surface-adsorbed oxygen means the rich surface oxygen vacancies. Generally, oxygen molecules in the reaction are activated by the abundant oxygen vacancies on the surface of the catalyst. Therefore, a high content of adsorbed oxygen species will increase the catalytic activity of the catalyst. As shown in Table 2, the percentage of O_{ads}/O_{latt} was 1.15, 0.99, 1.65, 1.19, and 1.10 on S-500, S-500(0.1), S-500(2.0), S-500(4.0), and S-500(2.0HCl), respectively. By comparison, the S-500(2.0) catalyst treated with 2 M NaOH solution has the highest proportion of surface-adsorbed oxygen species.

Furthermore, Figure 6C shows that the asymmetric peak of Fe 2p3/2 XPS and the peaks located at binding energies of 711.5, 714.8, and 718.5 eV can be attributed to Fe^{2+}, Fe^{3+} species and the satellite peaks of Fe^{2+} species on the surface of sludge-based catalysts, respectively.[17,26,27] The integrated peak area of Fe^{2+} and Fe^{3+} was calculated, as shown in Table 2. In comparison to other sludge-based catalysts, S-500(2.0) had the biggest molar percentage of Fe^{3+} species with 50.88%, which played a vital role in the adsorption of H_2S molecules.

In addition, it can be observed from the Ca 2p spectrum (Figure 6D) that the peak after alkaline treatment became significantly stronger, while the peak after acid treatment weakened significantly. The possible reason was that acid treatment can cause the washing of Ca on the surface of the material, while alkaline treatment can convert Ca into hydroxide and form calcium oxide on the surface of the material after calcination. Meanwhile, an obvious signal of Si 2p and Al 2p can be observed in Figure 6E, F.

3.6. Structure−Activity Relationship. The surface morphology, structure, physical−chemical properties, and surface chemical state of elements on the surface of the catalysts have a significant impact on their catalytic performance of H_2S selective oxidation. For sludge-based catalysts, the S-500 (2.0) catalyst treated with a 2 M NaOH solution has a larger proportion of external specific surface area and the smallest average particle size, which is beneficial for promoting the oxidation reaction of H_2S selective catalytic oxidation by enhancing the adsorption/activation sites of H_2S molecules; the surface adsorption oxygen on the catalyst is the main active oxygen species in the catalytic reaction of H_2S selective oxidation. Combined with the results of XPS and O_2-TPD, it can be seen that compared with the S-500 catalyst, the S-500(2.0) catalyst has much more oxygen vacancies and abundant surface adsorbed oxygen species, which is conducive to the conversion of HS^-. This may be one of the reasons that the S-500 (2.0) catalyst exhibits better catalytic performance of H_2S selective catalytic oxidation; in addition, from the XPS analysis results, it can be obtained that the S-500(2.0) catalyst has much more Fe^{3+} species, which is in favor of the adsorption and dissociation of H_2S, which may also be the reason for its higher catalytic activity; moreover, the S-500 (2.0) catalyst has a larger proportion of weak alkaline sites on its surface, which is conducive to the adsorption/dissociation of H_2S and the desorption of sulfur products. This is also considered to significantly improve the catalytic activity of the catalyst. Based on the characterization results and analysis, the excellent catalytic performance of H_2S selective oxidation on the S-500 (2.0) catalyst can be attributed to its larger external specific surface area, smaller average particle size, abundant oxygen vacancies, much more active oxygen species, more Fe^{3+}species, and a larger proportion of weakly alkaline sites.

4. CONCLUSIONS

1. In this work, a series of sludge-based catalysts are successfully prepared by adjusting the calcination temperature and the concentration of NaOH solution. Their application of H_2S selective catalytic oxidation is carried out. Evaluation results show that S-500 calcined at 500 °C performs better catalytic performance. S-500 treated with 2 M NaOH solution can obtain good H_2S removal efficiency while the catalytic performance of S-500 treated with 2 M HCl solution significantly decreased, indicating the important influence of acidity and alkalinity.
2. N_2-BET shows that S-500(2.0) has the biggest value of S_{ext}/S_{micro} and the bigger external specific surface area is in favor of the adsorption and diffusion of H_2S molecules, resulting in the improvement of H_2S selective catalytic oxidation on S-500(2.0); moreover, S-500(2.0) has the smallest average particle size of 11.17 nm, which is beneficial to the enrichment of more active sites, resulting in the enhancement of catalytic activity of H_2S selective oxidation; O_2-TPD implies that S-500(2.0) has the biggest value of O_{ads}/O_{Total} with 50.56%, suggesting that there are much more oxygen vacancies on S-500(2.0); CO_2-TPD indicates that the S-500(2.0) catalyst has the biggest $(CO_2)_{(weak+moderate)}/(CO_2)_{Total}$ ratio of 31.41%, indicating that S-500(2.0) has a larger proportion of weak alkaline sites on its surface, which is conducive to the adsorption/dissociation of H_2S and the desorption of sulfur products; XPS indicates that the S-500(2.0) catalyst has the highest proportion of adsorbed oxygen species and the biggest molar percentage of Fe^{3+} species with 50.88%.

AUTHOR INFORMATION

Corresponding Authors

Mingming Guo − *School of Environmental Science and Engineering, Shanghai Jiao Tong University, Shanghai 200240, P.R. China;* orcid.org/0000-0003-4331-0087; Email: mingmingguo@sjtu.edu.cn

Fangming Jin − *School of Environmental Science and Engineering, Shanghai Jiao Tong University, Shanghai 200240, P.R. China;* orcid.org/0000-0001-9028-8818; Email: fmjin@sjtu.edu.cn

Authors

Runtian He − *School of Environmental Science and Engineering, Shanghai Jiao Tong University, Shanghai 200240, P.R. China*

Xiaoyu Zhang − *School of Environmental Science and Engineering, Shanghai Jiao Tong University, Shanghai 200240, P.R. China*

Jia-nan Gu − *School of Environmental Science and Engineering, Shanghai Jiao Tong University, Shanghai 200240, P.R. China*

https://doi.org/10.1021/acsomega.4c03115
ACS Omega 2024, 9, 29691−29699

Kan Li − *School of Environmental Science and Engineering, Shanghai Jiao Tong University, Shanghai 200240, P.R. China;* orcid.org/0000-0002-1961-2459

Jinping Jia − *School of Environmental Science and Engineering, Shanghai Jiao Tong University, Shanghai 200240, P.R. China;* orcid.org/0000-0003-2409-338X

Tonghua Sun − *School of Environmental Science and Engineering, Shanghai Jiao Tong University, Shanghai 200240, P.R. China;* orcid.org/0000-0003-3803-0232

Complete contact information is available at: https://pubs.acs.org/10.1021/acsomega.4c03115

Notes

The authors declare no competing financial interest.

■ ACKNOWLEDGMENTS

This work was supported by the National Natural Science Foundation of China (Grant No. 22076118).

■ REFERENCES

(1) Rahimi, Z.; Zinatizadeh, A. A.; Zinadini, S.; van Loosdrecht, M.; Batstone, D. J. Concurrent removal of carbon and nutrients in a one-stage dual internal circulation airlift A_2O bioreactor from milk processing industrial wastewater: Process optimization, sludge characteristics and operating cost evaluation. *Chemosphere* **2024**, *355*, No. 141804, DOI: 10.1016/j.chemosphere.2024.141804.

(2) Traina, F.; Capodici, M.; Torregrossa, M.; Viviani, G.; Corsino, S. F. PHA and EPS production from industrial wastewater by conventional activated sludge, membrane bioreactor and aerobic granular sludge technologies: A comprehensive comparison. *Chemosphere* **2024**, *355*, No. 141768.

(3) Ji, X.; Zhu, M.; Li, M.; Wang, N.; Li, M.; Song, L.; Shan, R. Adsorption and Degradation of Organics in Wastewater on Municipal Sludge. *ACS Omega* **2023**, *8* (37), 33349−33357.

(4) Wang, Z.; Gao, B.; Liu, J.; Sillanpää, M.; Kim, Y. The oxidation treatment of pharmaceutical wastewater in H_2O_2 and PMS system by Iron-containing biochar originated from excess sludge. *J. Water Process Eng.* **2024**, *58*, No. 104833.

(5) Duan, J.; Kitamura, K.; Tsukamoto, H.; Van Phan, H.; Oba, K.; Hori, T.; Fujiwara, T.; Terada, A. Enhanced granulation of activated sludge in an airlift reactor for organic carbon removal and ammonia retention from industrial fermentation wastewater: A comparative study. *Water Res.* **2024**, *251*, No. 121091.

(6) Pasciucco, E.; Pasciucco, F.; Iannelli, R.; Pecorini, I. A Fenton-based approach at neutral and un-conditioned pH for recalcitrant COD removal in tannery wastewater: Experimental test and sludge characterization. *Sci. Total Environ.* **2024**, *926*, No. 172070.

(7) Pan, K.; Guo, T.; Liao, H.; Huang, Z.; Qian, Z.; Li, F.; Li, J. Adding iron shavings in activated sludge system to enhance removal of refractory organics and nitrogen for textile-dyeing wastewater. *J. Environ. Chem. Eng.* **2023**, *11* (5), No. 110999.

(8) Pan, Z.; Wei, H.; Qiu, C.; Yang, Q.; Liang, Y.; Huang, Z.; Li, J. Two-stage sequencing batch reactors with added iron shavings for nutrient removal and aerobic sludge granulation treating real wastewater with low carbon to nitrogen ratios. *Bioresour. Technol.* **2024**, *396*, No. 130380.

(9) Sun, F.; Lu, D.; Ho, J. S.; Chong, T. H.; Zhou, Y. Mitigation of membrane fouling in a seawater-driven forward osmosis system for waste activated sludge thickening. *J. Cleaner Prod.* **2019**, *241*, No. 118373.

(10) Zhou, G.; Gu, Y.; Yuan, H.; Gong, Y.; Wu, Y. Selecting sustainable technologies for disposal of municipal sewage sludge using a multi-criterion decision-making method: A case study from China. *Resour., Conserv. Recycl.* **2020**, *161*, No. 104881.

(11) Guo, Y.; Zhang, X.; Zhang, D.; Li, S.; Wang, H.; Peng, Y.; Bian, Z. Catalysts containing Fe and Mn from dewatered sludge showing enhanced electrocatalytic degradation of triclosan. *Environ. Res.* **2022**, *214*, No. 114065.

(12) Che, L.; Yang, B.; Tian, Q.; Xu, H. Iron-based biochar derived from waste-activated sludge enhances anaerobic digestion of synthetic salty organic wastewater for methane production. *Bioresour. Technol.* **2022**, *345*, No. 126465.

(13) Xu, T.; Wang, L. a.; Wu, H.; Jiang, D.; Qi, N.; Gou, Z. Municipal solid waste incineration (MSWI) fly ash could be used as a catalyst for pyrolysis of oil-based drill cuttings from shale gas exploitation industry. *J. Cleaner Prod.* **2023**, *387*, No. 135754.

(14) Zhang, H.; Chen, S.; Zhang, N.; Chen, H.; Yang, Y.; Tu, Y.; Jiao, C.; Xu, Z.; Xia, Y.; Suo, H.; et al. Sewage Sludge-Derived catalyst for extremely efficient electrocatalytic elimination of organic pollutants in water. *Chem. Eng. J.* **2023**, *469*, No. 143777.

(15) Tian, X.; Chen, Y.; Chen, Y.; Chen, D.; Wang, Q.; Li, X. Removal of Gaseous Hydrogen Sulfide by a $FeOCl/H_2O_2$ Wet Oxidation System. *ACS Omega* **2022**, *7* (9), 8163−8173.

(16) Shi, L.; Yang, K.; Zhao, Q.; Wang, H.; Cui, Q. Characterization and Mechanisms of H_2S and SO_2 Adsorption by Activated Carbon. *Energy Fuels* **2015**, *29* (10), 6678−6685.

(17) Xiong, Y.; Wang, L.; Ning, P.; Luo, J.; Li, X.; Yuan, L.; Xie, Y.; Ma, Y.; Wang, X. Constructing oxygen vacancy-enriched Fe_3O_4@MnO_2 core−shell nanoplates for highly efficient catalytic oxidation of H_2S in blast furnace gas. *Sep. Purif. Technol.* **2024**, *336*, No. 126234.

(18) Li, S.; Fu, H.; Zhang, X.; Liu, X.; Tuci, G.; Giambastiani, G.; Pham-Huu, C.; Liu, Y. Hierarchically porous, N-defect enriched C-nanosheets boost the H_2S selective oxidation to elemental sulfur. *Appl. Catal., B* **2024**, *343*, No. 123505.

(19) Yang, C.; Ye, H.; Byun, J.; Hou, Y.; Wang, X. N-Rich Carbon Catalysts with Economic Feasibility for the Selective Oxidation of Hydrogen Sulfide to Sulfur. *Environ. Sci. Technol.* **2020**, *54* (19), 12621−12630.

(20) Zheng, X.; Li, B.; Shen, L.; Cao, Y.; Zhan, Y.; Zheng, S.; Wang, S.; Jiang, L. Oxygen vacancies engineering of Fe doped $LaCoO_3$ perovskite catalysts for efficient H_2S selective oxidation. *Appl. Catal., B* **2023**, *329*, No. 122526.

(21) Huan, C.; Fang, J.; Tong, X.; Zeng, Y.; Liu, Y.; Jiang, X.; Ji, G.; Xu, L.; Lyu, Q.; Yan, Z. Simultaneous elimination of H_2S and NH_3 in a biotrickling filter packed with polyhedral spheres and best efficiency in compost deodorization. *J. Cleaner Prod.* **2021**, *284*, No. 124708.

(22) Vikromvarasiri, N.; Juntranapaporn, J.; Pisutpaisal, N. Performance of Paracoccus pantotrophus for H_2S removal in biotrickling filter. *Int. J. Hydrogen Energy* **2017**, *42* (45), 27820−27825.

(23) Yang, C.; Wang, J.; Fan, H.-L.; Shangguan, J.; Mi, J.; Huo, C. Contributions of tailored oxygen vacancies in ZnO/Al_2O_3 composites to the enhanced ability for H_2S removal at room temperature. *Fuel* **2018**, *215*, 695−703.

(24) Phatyenchuen, S.; Pongthawornsakun, B.; Panpranot, J.; Praserthdam, P. Effect of transition metal dopants (M= Nb, La, Zr, and Y) on the M-TiO_2 supported V_2O_5 catalysts in the selective oxidation of H2S to elemental sulfur. *Journal of Environmental Chemical Engineering* **2018**, *6* (5), 5655−5661.

(25) Li, L.; Sun, T. H.; Shu, C. H.; Zhang, H. B. Low temperature H_2S removal with 3-D structural mesoporous molecular sieves supported ZnO from gas stream. *Journal of Hazardous Materials* **2016**, *311*, 142−150.

(26) Gu, J.-N.; Liang, J.; Xue, Y.; Yu, C.; Li, X.; Li, K.; Guo, M.; Jia, J.; Sun, T. Highly Dispersed FeAg-MCM41 Catalyst for Medium-Temperature Hydrogen Sulfide Oxidation in Coke Oven Gas. *Environ. Sci. Technol.* **2023**, *57* (36), 13579−13587.

(27) Zhang, F.; Zhang, X.; Jiang, G.; Li, N.; Hao, Z.; Qu, S. H_2S selective catalytic oxidation over Ce substituted $La_{1-x}Ce_xFeO_3$ perovskite oxides catalyst. *Chemical Engineering Journal* **2018**, *348*, 831−839.